



Cite this: *Environ. Sci.: Water Res. Technol.*, 2019, 5, 564

## Degradation of ciprofloxacin by 185/254 nm vacuum ultraviolet: kinetics, mechanism and toxicology†

Han Hu,<sup>a</sup> Ya Chen,<sup>a</sup> Jinshao Ye,<sup>ab</sup> Li Zhuang,<sup>a</sup> Hongling Zhang<sup>a</sup> and Huase Ou <sup>\*a</sup>

Fluoroquinolone antibiotics (FQs) are highly resistant to conventional biological water treatment processes, thus, it is desirable to develop novel water treatment methods for eliminating FQs efficiently. Vacuum ultraviolet (VUV; 185/254 nm) may be a novel alternative due to its capacity of photolyzing water into hydroxyl radicals without chemical addition. Ciprofloxacin (CIP) was selected as the representative of FQs, and its degradation using VUV treatment was tested. A first-order reaction kinetics with a rate constant ( $k_{app}$ ) at  $8.78 \times 10^{-3} \text{ s}^{-1}$  was observed when  $[CIP]_0 = 3.02 \text{ }\mu\text{M}$  and 185 nm irradiation intensity =  $0.12 \text{ mW cm}^{-2}$ . Wavelength screening, radical scavenging and kinetic calculations revealed that direct photolysis and indirect radical-based oxidation both contributed to the degradation, with a reaction rate constant ( $k_{OH-CIP}$ ) at  $(8.6 \pm 0.8) \times 10^9 \text{ M}^{-1} \text{ s}^{-1}$ . Radical-based addition, substitution and cleavage of CIP generated five series of stable products. Most products in the early stage were simple hydroxylated intermediates from CIP. Based on the toxicology analysis including reactive oxygen species and apoptosis of *Escherichia coli*, these early-stage products were supposed to have higher toxicity than CIP. However, as they were transformed into further oxidized products, their toxicity was reduced. Variable pH values and natural organic matter/anions significantly affected the degradation efficiency. Altogether, VUV induced the rapid degradation of CIP, and it will be a promising treatment method for transforming and detoxifying micro-pollutants from water.

Received 21st October 2018,  
Accepted 14th January 2019

DOI: 10.1039/c8ew00738a

rs.li/es-water

### Water impact

This study provides insights into the performance of vacuum ultraviolet (VUV) on the removal of ciprofloxacin (CIP). Degradation kinetics, mechanisms, products, pathways and toxicity variation were evaluated. The current study revealed that the incomplete hydroxylation products likely have higher toxicities than their parent CIP, and further mineralization of them into inorganic matter will be required for complete detoxification. This study provides useful information with regards to the potentiality of chemical-addition-free VUV for effectively eliminating and detoxifying organic pollutants from water.

## 1. Introduction

Fluoroquinolone antibiotics (FQs) are intensively used for human (domestic and hospital use), veterinary and agriculture purposes. The most common FQs are ciprofloxacin (CIP), ofloxacin and norfloxacin, which have been detected in environments worldwide.<sup>1</sup> After application, a portion of FQs are discharged into sewer systems. FQs are designed to be biologically resistant, thus, conventional biological wastewater treatment plants (WWTPs) have poor performance on their elimination, and sorption of FQs into sewage sludge has been

confirmed to be the pre-dominant removal mechanism.<sup>2–4</sup> Residual FQs are continuously released with WWTP effluent and excess sludge. Municipal WWTPs are therefore considered as one of the main sources of FQs for receiving water bodies and lands.<sup>5</sup> Numerous researchers have found that FQs in the environment aggravated several ecological problems, such as the increase of antibiotic resistance of bacteria,<sup>6</sup> the physiological teratogenesis of plants/algae<sup>7</sup> and the chronic genotoxicity/carcinogenic potential to organisms.<sup>8</sup> Thus, it is desirable to develop novel water treatment methods for eliminating FQs efficiently.

FQs all have a common quinoline structure, giving their characteristic absorption at ultraviolet (UV) wavelengths. Thus, UV irradiation, especially UV-C, induces direct photolysis of FQs with low reaction rates. Of note, irradiation at the optimal UV wavelength can improve the photolysis efficiency. For example, the maximum absorption of CIP is 280 nm, at which the fastest UV photolysis can be achieved.<sup>9</sup> To improve

<sup>a</sup> School of Environment, Guangdong Key Laboratory of Environmental Pollution and Health, Jinan University, Guangzhou 510632, China.

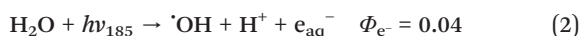
E-mail: touhuase@jnu.edu.cn; Tel: +86 020 37278961

<sup>b</sup> Joint Genome Institute, Lawrence Berkeley National Laboratory, Walnut Creek 94598, CA, USA

† Electronic supplementary information (ESI) available. See DOI: 10.1039/c8ew00738a

the removal efficiency, UV-based advanced oxidation processes (UV-AOPs), such as UV/H<sub>2</sub>O<sub>2</sub>, UV/persulfate and UV/TiO<sub>2</sub>, have been tested. Generation of highly oxidative radicals in UV-AOPs can degrade and even mineralize FQs rapidly under mild conditions. Early studies explored and compared the basic kinetics of direct UV photolysis and UV/H<sub>2</sub>O<sub>2</sub> oxidation.<sup>10,11</sup> Kinetics parameters, such as quantum yield and degradation mechanisms, were further investigated.<sup>12,13</sup> Lately, research studies of FQ degradation using UV/persulfate or UV/peroxymonosulfate have proved its efficiency.<sup>14</sup> Serna-Galvis *et al.*<sup>15</sup> compared the degradation of several FQs using sole-UV and UV/persulfate, and found that the contribution ratios of direct photolysis and radical oxidation varied with different FQs. In our previous study, incomplete degradation of CIP with UV/persulfate was suggested to be likewise efficient for detoxification.<sup>16</sup> As UV/H<sub>2</sub>O<sub>2</sub> and UV/persulfate require repeated addition, UV/TiO<sub>2</sub> photocatalysis may be a more sustainable alternative.<sup>17–19</sup> However, challenges for the applications of these UV-AOPs still exist, such as the addition of chemical agents and the control of operational conditions.

Vacuum ultraviolet (VUV; 100–200 nm) may be a novel alternative UV-AOP due to its capacity of photolyzing water into hydroxyl radicals ( $\cdot\text{OH}$ , quantum yield  $\Phi$  at 0.33) without chemical additions (eqn (1) and (2)).<sup>20</sup> Reaction mechanisms of micro-pollutants (MPs) in VUV systems likewise involve photolysis and radical oxidation. VUV can degrade phenols,<sup>21</sup> chlorinated hydrocarbons,<sup>22</sup> perfluorinated compounds,<sup>23</sup> pesticides,<sup>24</sup> *etc.* There are only a few research studies focused on the degradation of MPs using VUV systems. Imoberdorf and Mohseni<sup>25</sup> developed a kinetic model, which took into account basic degradation mechanisms, for the prediction of degradation processes of 2,4-dichlorophenoxyacetic acid in a VUV photoreactor. Li *et al.*<sup>26</sup> established a mini-fluidic VUV/UV photoreaction system which emitted a 185/254 nm or sole 254 nm beam with a nearly identical UV intensity. In their later studies, several key photochemical kinetic parameters (*e.g.*, photon fluence-based rate constant and quantum yield) of MPs were determined.<sup>27,28</sup> Gu *et al.*<sup>23</sup> used VUV/sulfite to degrade perfluorooctane sulfonate with an overall apparent rate constant at 0.015 min<sup>-1</sup>. These initial studies provided basic data and methodology for the research about MPs under VUV treatment. Still, there is no research about the degradation of any FQs with VUV, not to mention their degradation mechanism, mineralization efficiency and toxicology evaluation.<sup>29</sup>



In this study, CIP was selected as the representative of FQs. Degradation mechanisms and kinetics were identified based on wavelength screening and radical scavenging with a customized VUV device. The evolution pathway and toxicity variation of CIP degradation products were determined. High-resolution mass spectrometry (HRMS) was applied, and

analyses of oxygen species (ROS) and cellular apoptosis based on model organism *Escherichia coli* were conducted. Crucial inhibition effects on VUV systems were also estimated by influence factor experiments with variable pH values, natural organic matter (NOM) and anions.

## 2. Materials and methods

### 2.1. Chemical reagents

CIP (99%, HPLC grade), ethyl alcohol (EtOH, HPLC grade), *tert*-butyl alcohol (TBA, HPLC grade), formic acid (99%, HPLC grade), ascorbic acid (99%) and humic acid (HA) (90% dissolved organic matter, CAS: 1415-93-6) were purchased from Sigma-Aldrich (USA). Methanol (HPLC grade) and acetonitrile (HPLC grade) were obtained from Fisher (USA). NaNO<sub>3</sub> (98%), NaCl (98%), Na<sub>2</sub>CO<sub>3</sub> (98%), Na<sub>2</sub>SO<sub>4</sub> (98%), KH<sub>2</sub>PO<sub>4</sub> (98%) and NaHCO<sub>3</sub> (98%) were purchased from Sinopharm (China). Solutions were prepared using 18.2 MΩ ultrapure water as the matrix. Other chemical reagents were of the highest purity available.

### 2.2. VUV irradiation experiments

A VUV quasi-parallel irradiation device, which included a framework, a VUV lamp and a reactor vessel, was designed (Fig. S1, ESI;† “S” designates texts, tables, figures and other contents in the ESI thereafter). The reactor framework was designed and made by 3D laser rapid prototyping. Filling of N<sub>2</sub> gas was applied inside the device to avoid the absorption of 185 nm VUV irradiation. The VUV low-pressure argon–mercury lamp emitted both 185 nm and 254 nm irradiation. Based on the product instruction from the lamp supplier, 185 nm and 254 nm contributed 6% and 94%, respectively, to the total light intensity. The actual intensity of 254 nm on the surface of CIP solution was determined using a 254 nm photometer, while an actual intensity of 185 nm irradiation was calculated based on it. By changing the distance between the solution surface and lamp, the irradiation intensity can be adjusted. Customized circular quartz vessels with a diameter of 12 cm were applied. A given volume (typical 20–100 mL) of CIP solution (typical [CIP]<sub>0</sub> = 3.02 μM) was added into the reactor vessel. Before reaction, solution pH was adjusted using buffered solution with different concentration combinations of NaOH, KH<sub>2</sub>PO<sub>4</sub> and H<sub>3</sub>PO<sub>4</sub>. The reaction solution was orbitally shaken at 60 rpm on a fixed heating platform at 25 ± 2 °C. After turning on the VUV light source, the treated samples (2 mL in normal experiments) were obtained at the pre-set times, and then transferred into brown amber tubes and stored at 4 °C before analysis. In the experiments in which the samples were prepared for subsequent microbial culture and pollutant exposure experiments, a total of 10 group samples (100 mL) were used for the VUV treatment, and then only 20 mL solution was obtained at the pre-set times one by one from the treated samples.

For the wavelength screening experiment, coverage of a JGS2 fused silica wafer was applied on top of the reaction solution. JGS2 silica can filter light irradiation below 200

nm, but most 254 nm irradiation can penetrate through JGS2 silica. Thus, it can be used to screen 185 nm and leave behind 254 nm from the VUV lamp. By this means, the functions of 185 nm and 254 nm can be separated. To determine the radical oxidation, several scavenger species were added with a concentration at 100 mM. In the influence factor experiments, predetermined amounts of HA or inorganic anions were mixed into the reaction solution.

### 2.3. Analysis of CIP and its degradation products

Quantitative analysis of CIP was conducted by HPLC/MS<sup>2</sup> (TripleQuad 5500, Applied Biosystems SCIEX, USA). Qualitative analysis of its degradation products was performed using a TripleTOF 5600+ HRMS (Applied Biosystems SCIEX, USA). The relative intensities (peak areas) of the organic degradation products were obtained by HPLC/MS<sup>2</sup>. Detailed analysis processes are presented in Text S1 and Table S1.† Total organic carbon (TOC) was analyzed using a TOC-L analyzer (Shimadzu, Japan). Determination of NO<sub>3</sub><sup>-</sup> and F<sup>-</sup> was performed using an ICS-2500 analyzer (Dionex, USA). An ED50A detector and a DIONEX IonPac® AS15 column were used, and 30.0 mM NaOH solution was applied as the mobile phase.

### 2.4. Kinetics calculation

In the VUV system, 185 nm photolysis, 254 nm photolysis and ·OH oxidation may synchronously degrade CIP. The kinetics equation of CIP can be presented as:

$$-\frac{d[\text{CIP}]}{dt} = (k_{185-d} + k_{254-d} + k_{\text{OH-CIP}} \times [\cdot\text{OH}]) \times [\text{CIP}] = k_{\text{app}} \times [\text{CIP}] \quad (3)$$

where,  $k_{185-d}$  and  $k_{254-d}$  represent the reaction rate constants of direct photolysis induced by 185 nm and 254 nm irradiation, respectively;  $k_{\text{OH-CIP}}$  represents the second-order reaction rate between ·OH and CIP. The reaction rate in the sole UV system with an identical UV intensity at 254 nm follows:

$$-\frac{d[\text{CIP}]}{dt} = k_{254-d} \times [\text{CIP}] = k_{\text{app}} \times [\text{CIP}] \quad (4)$$

Setting CIP as the targeted contaminant (T),  $k_{\text{OH-CIP}}$  was calculated according to competition kinetics in a binary mixture with *para*-chlorobenzoic acid (*p*CBA) as the reference compound (R).<sup>12</sup> As the reaction rate constant between ·OH and the reference compounds ( $k_{\text{R}}$ ;  $k_{\text{OH-pCBA}} = 5.0 \times 10^9 \text{ M}^{-1} \text{ s}^{-1}$ ) is already known, the ·OH reaction rate constant with CIP ( $k_{\text{T}}$ ;  $k_{\text{OH-CIP}}$ ) was calculated by:<sup>30</sup>

$$\ln\left(\frac{[\text{T}]}{[\text{T}]_0}\right) = \frac{k_{\text{T}}}{k_{\text{R}}} \ln\left(\frac{[\text{R}]}{[\text{R}]_0}\right) \quad (5)$$

This equation does not consider the direct photolysis. Thus, there will be an overestimation of  $k_{\text{OH-CIP}}$  based on the calculation of this equation.

### 2.5. Molar absorption coefficients and apparent quantum yields

Molar absorption coefficients ( $\epsilon$ ) of CIP, scavengers and anion solutions were calculated based on the UV absorbance (180–280 nm) determined using a Chirascan circular dichroism spectrometer (Applied Photophysics, UK). For the spectrum at 185 nm, the analysis was performed under N<sub>2</sub> purging to avoid the optical absorption of O<sub>2</sub>. Cuvettes with 1, 5 and 10 mm light path lengths were applied. The  $\epsilon$  of these solutions can be used to calculate the distribution of photons in a specific mixed solution system. For example, the percentage of 185 nm photons absorbed by a particular constituent in this system can be calculated by:<sup>24</sup>

$$\%185 \text{ nm} = \frac{C_i \epsilon_i}{\sum_{i=1}^N C_i \epsilon_i} \quad (6)$$

where  $C_i$  represents the concentration of constituent  $i$ , and  $\epsilon_i$  represents the absorption coefficient of constituent  $i$ . The percentage of 254 nm irradiation follows a similar formula. Apparent quantum yields of CIP at 185 nm and 254 nm were calculated following similar processes to those in ref. 24.

### 2.6. Microbial culture and pollutant exposure

*Escherichia coli* was inoculated with 100 mL lysogeny broth medium in 250 mL Erlenmeyer flasks, which were orbitally shaken at 160 r min<sup>-1</sup> (37 °C; 12 h). The cultured cells were separated by centrifugation at 6000g (10 min), and then they were washed three times with sterile phosphate buffer. Bacterial suspension containing the separated cells at 1.0 g L<sup>-1</sup> initial biomass dosage in 20 mL M9 medium was prepared. Solutions with 3.02 μM CIP (the control group) or the mixture of the degradation products after VUV reactions (the treated group, reaction conditions were the same as those in section 2.2) were mixed with the bacterial suspension with a volume ratio at 1:1. All these mixed bacterial suspensions were cultured at 37 °C on a rotary shaker at 160 r min<sup>-1</sup> in the dark. After 6 h exposure of the culture, the samples were collected and taken for ROS, MP and apoptosis analyses immediately.<sup>31</sup> Each treatment had three replicates. Detailed analysis procedure is listed in Text S2.†

## 3. Results and discussion

### 3.1. Degradation efficiency

Sole UV-C (using a low-pressure mercury lamp emitting 254 nm) and UV-C/VUV (using a VUV lamp emitting 254 nm + 185 nm) treatments with the same intensity at 254 nm (0.8 mW cm<sup>-2</sup>) for CIP degradation were conducted (Fig. 1a). In the UV-C and UV-C/VUV systems, the degradation of CIP followed first-order reaction kinetics with rate constants ( $k_{\text{app}}$ ) at  $1.24 \times 10^{-3} \text{ s}^{-1}$  and  $8.78 \times 10^{-3} \text{ s}^{-1}$ , respectively. Compared to 53% in the sole UV-C system, approximately 99% CIP was transformed within 10 min of VUV + UV-C treatment.

The variation of UV irradiation intensity significantly affected the reaction efficiency of the UV-C/VUV system. An approximately positive linear correlation between the VUV intensity and  $k_{\text{app}}$  was observed, with an increasing  $k_{\text{app}}$  from  $1.22 \times 10^{-3} \text{ s}^{-1}$  to  $8.78 \times 10^{-3} \text{ s}^{-1}$  as the 185 nm intensity raised from  $0.015 \text{ mW cm}^{-2}$  to  $0.12 \text{ mW cm}^{-2}$  (Fig. 1b). The increasing VUV intensity enhances the yield of  $\cdot\text{OH}$ , resulting in higher reaction efficiency. The reaction using  $0.12 \text{ mW cm}^{-2}$  at 185 nm was selected as the control group in section 3.2.

### 3.2. Mechanisms and kinetics

To reveal the major contributor to CIP removal, optical screening with JGS-2 silica was performed (Fig. 1a). JGS-2 silica screens UV irradiation with a wavelength less than 200 nm, thus, only 254 nm UV can penetrate and 185 nm UV is screened. After adding JGS-2 silica, the degradation rate of CIP using the VUV lamps reduced to a similar level ( $k$  at  $1.40 \times 10^{-3} \text{ s}^{-1}$ ) as that using sole UV-C lamp, suggesting that the promotion can be attributed to 185 nm irradiation.

Three mechanisms, including 185 nm photolysis, 254 nm photolysis and  $\cdot\text{OH}$  oxidation, may contribute to the transformation of CIP synchronously (eqn (3)). To determine the kinetic parameters in eqn (3) and the degradation mechanisms, a series of deliberately designed experiments were conducted. Both 185 nm and 254 nm irradiation can induce direct photolysis, whose efficiencies mainly depend on the photon energy absorbed by CIP. Water has a high  $\epsilon$  at 185 nm ( $1.8 \text{ cm}^{-1}$ ), while anions and organic matter all have high light absorption efficiencies at 185 nm but not at 254 nm (Table S2†). Approximately 5 mm thickness of ultrapure water can absorb approximately 90% of the 185 nm ultraviolet.<sup>32</sup> In the current study, 185 nm irradiation intensity only occupied 6% in the total intensity of the VUV lamp, and the reaction solution reached 15 mm depth, which can absorb most of

the 185 nm irradiation. The percentage of 185 nm photons absorbed by CIP was calculated using eqn (6). For  $3.02 \mu\text{M}$  CIP in ultrapure water, 3.0% and 97.0% of 185 nm photons were absorbed by CIP and water, respectively. Therefore, it can be concluded that direct photolysis induced by 185 nm irradiation may play a minor role in CIP degradation, and eqn (3) can be simplified to:

$$-\frac{d[\text{CIP}]}{dt} = (k_{254-d} + k_{\text{OH-CIP}} \times [\cdot\text{OH}]) \times [\text{CIP}] = k_{\text{app}} \times [\text{CIP}] \quad (7)$$

In contrast, 254 nm irradiation induced significant photolysis of CIP. As the intensity at 254 nm in the UV-C and VUV systems was in both cases at  $0.8 \text{ mW cm}^{-2}$ , the direct photolysis of CIP by 254 nm irradiation in both systems followed eqn (4) with the same rate constant at  $1.24 \times 10^{-3} \text{ s}^{-1}$ . The apparent quantum yield for 254 nm UV-C photolysis ( $\Phi_{254}$ ) was calculated to be  $0.004 \pm 0.0003$  (Table 1).

Most of the 185 nm irradiation would be absorbed by water which is transformed into  $\cdot\text{OH}$ . Radical-based oxidation would thus be the dominant mechanism for CIP degradation. To further confirm the radical-based oxidation, addition of typical radical scavengers was applied. After adding 10 mM ascorbic acid, removal efficiency was severely inhibited as the  $k_{\text{app}}$  decreased from  $8.78 \times 10^{-3} \text{ s}^{-1}$  to  $0.29 \times 10^{-3} \text{ s}^{-1}$ . Ascorbic acid is a strong reductant and can scavenge most of the oxidants, indicating that the degradation of CIP was dominated by oxidation. However, ascorbic acid has a high  $\epsilon$  value ( $3130 \pm 184 \text{ M}^{-1} \text{ cm}^{-1}$ ) at 185 nm (Table S2†). Besides oxidant scavenging, screening effect on 185 nm irradiation may also result in this inhibition. To exclude the screening effect and further confirm the role of reactive species, EtOH and TBA were added. EtOH and TBA have weak VUV screening effects with  $\epsilon$  at  $(31.31 \pm 5.3) \text{ M}^{-1} \text{ cm}^{-1}$  and  $(14.72 \pm 2.1) \text{ M}^{-1} \text{ cm}^{-1}$

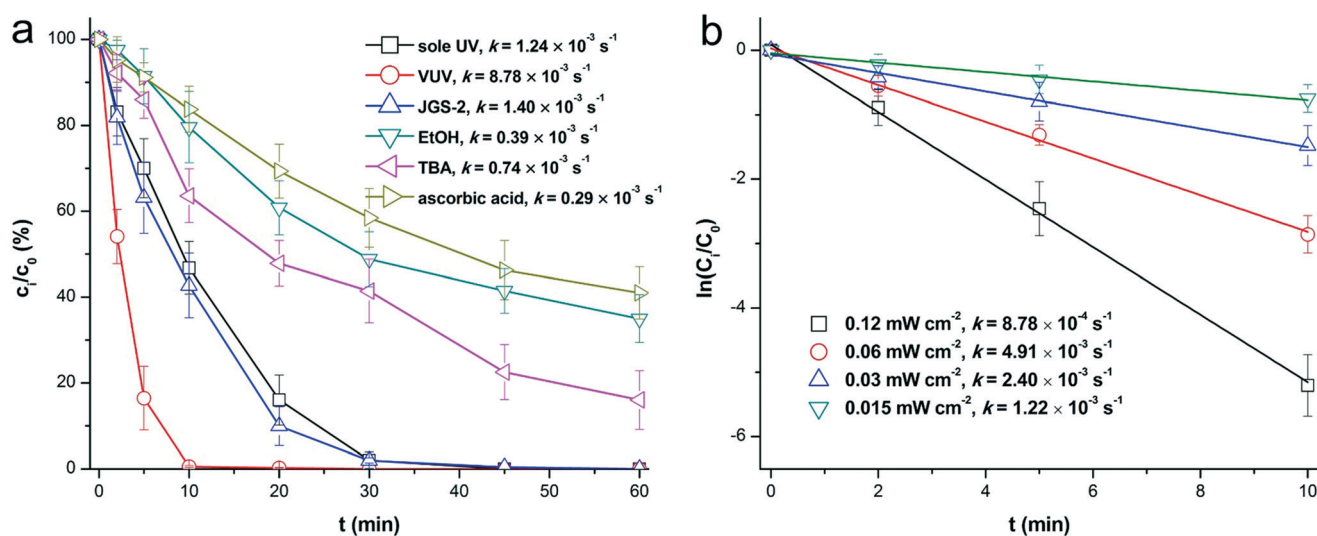


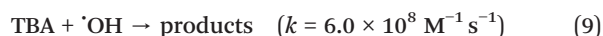
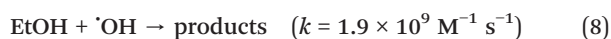
Fig. 1 Degradation efficiency of CIP with scavengers (a) and different VUV intensities (b). Experimental conditions: solution temperature  $25 \pm 2 \text{ }^\circ\text{C}$ , pH 6.5–7.2,  $[\text{CIP}]_0 = 3.02 \mu\text{M}$ , 185 nm VUV irradiation intensity =  $0.12 \text{ mW cm}^{-2}$  (if not specified). All the experiments were carried out in triplicate with error bars representing the standard error of the mean.

**Table 1** Kinetics parameters for CIP

Irradiation intensity (mW cm <sup>-2</sup> )	Sole UV		VUV		
	$k_{254}$ (s <sup>-1</sup> )	$\Phi_{254-d}$	$k_{app}$ (s <sup>-1</sup> )	$k_{OH-CIP}$ (M <sup>-1</sup> s <sup>-1</sup> )	$\Phi_{185}$
2.0	$(1.24 \pm 0.13) \times 10^{-3}$	$0.004 \pm 0.0003$	$(8.78 \pm 0.61) \times 10^{-3}$	$(8.6 \pm 0.8) \times 10^9$	$0.18 \pm 0.02$

Experimental conditions: solution temperature  $25 \pm 2$  °C, pH 6.5–7.2, [CIP]<sub>0</sub> = 3.02 μM, 254 nm UV irradiation intensity = 2.0 mW cm<sup>-2</sup>, 185 nm VUV irradiation intensity = 0.12 mW cm<sup>-2</sup>.

(185 nm), respectively, and they have strong scavenging capacities for ·OH (eqn (8) and (9)). After adding these two scavengers,  $k_{app}$  reduced significantly to  $0.39 \times 10^{-3}$  s<sup>-1</sup> and  $0.74 \times 10^{-3}$  s<sup>-1</sup>, suggesting that ·OH oxidation might be the predominant contributor for the CIP degradation in the VUV system.



As *p*CBA has a low UV absorption and moderate reaction rate with ·OH, a competitive reaction with *p*CBA was performed to determine relevant kinetic parameters. The  $k_{OH-pCBA}$  was calculated to be  $5.0 \times 10^9 \text{ M}^{-1} \text{ s}^{-1}$ ,<sup>33</sup> and the second-order rate constant ( $k_{OH-CIP}$ ) was calculated to be  $(8.6 \pm 0.8) \times 10^9 \text{ M}^{-1} \text{ s}^{-1}$ . Some other researchers have explored the  $k_{OH-CIP}$ . Yuan *et al.*<sup>34</sup> and Keen *et al.*<sup>12</sup> investigated the degradation efficiencies of CIP in a UV/H<sub>2</sub>O<sub>2</sub> system, and *p*CBA was also used to determine  $k_{OH-CIP}$  with results at  $7.5 \times 10^9 \text{ M}^{-1} \text{ s}^{-1}$  and  $7.8 \times 10^9 \text{ M}^{-1} \text{ s}^{-1}$ , respectively. An *et al.*<sup>35</sup> evaluated the degradation kinetics and mechanisms of CIP in UV/TiO<sub>2</sub>, and determined a lower  $k_{OH-CIP}$  at  $(2.1 \pm 0.1) \times 10^9 \text{ M}^{-1} \text{ s}^{-1}$ . Dodd *et al.*<sup>36</sup> used ozonation for CIP degradation, and they found that  $k_{OH-CIP}$  was  $(4.1 \pm 0.3) \times 10^9 \text{ M}^{-1} \text{ s}^{-1}$ . The difference between the current study and the previous ones can be attributed to the different reference compounds applied or the different treatment methods. Of note, since the 254 nm photolysis was ignored during competitive reaction calculations, the  $k_{OH-CIP}$  obtained here was somewhat overestimated. Furthermore, the apparent quantum yield for 185 nm VUV treatment ( $\Phi_{185}$ , mainly ·OH oxidation) was calculated to be  $0.18 \pm 0.02$ . This relatively high  $\Phi_{185}$  may be due to the high photolysis efficiency of H<sub>2</sub>O to ·OH (0.33) under 185 nm irradiation.

### 3.3. Mineralization, degradation intermediates and pathways

An initial TOC value at 0.65 mg L<sup>-1</sup> was detected for 3.02 μM CIP, and an evident decrease (>40%) was observed during 60 min of VUV treatment (Fig. S2†). This moderate mineralization efficiency indicated that VUV induced incomplete transformation of CIP, thus, a variety of degradation products were generated. Based on the potential transformation pathways of CIP, five series of stable products, including product A (site 1), product B (site 5), product C (site 6),

product D (site 10) and product E (sites 11–14), were identified by HRMS (Table 2). Since there is no standard substance for these products, they can only be classified as tentative candidates. There are several general routes that ·OH reacts with heterocyclic organic pollutants. Dionysiou *et al.*<sup>37–39</sup> reported that main reaction mechanisms may involve a series of additions, substitutions and cleavages on different sites of targeted contaminants. Based on these studies, the degradation pathways of CIP are presented in Fig. 2, and the relative intensity variations of its products were determined (Fig. 3).

Product A-1 was generated upon substitution of the fluoride atom at site 1 by a hydroxyl, and then further addition of another hydroxyl at site 6 may lead to the generation of product A-2. The replacement of a carboxyl by a hydroxyl at site 5 generated product B. A hydroxyl was added onto site 6, resulting in the generation of product C-1. The cleavage of the double bond in the quinolone ring and the further oxidation of C-1 resulted in transformation to products C-2 and C-3. Product D was generated by the cleavage of piperazine ring, while products E-1-1 and E-2-1 were generated by the modifications on them. Of note, elimination of the hydroxyl may occur on sites 13 and 14 of E-2-1, in which a double bond can be formed (product E-2-2), and further addition of hydroxyl in E-2-2 may generate product E-2-3. Additions of hydroxyl radicals on other sites of product E-2-1 may lead to product E-2-4. Generally, a product mixture was generated by photolysis and ·OH oxidation, while sites 1, 5, 6, 10–14 were susceptible in the VUV system.

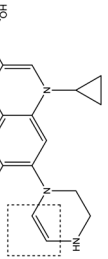
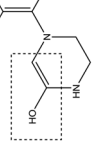
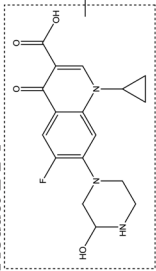
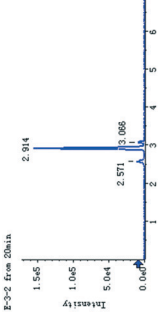
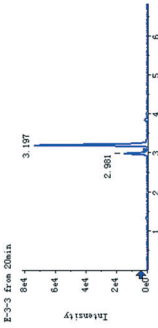
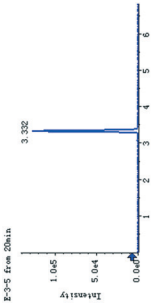
Reactive radicals in other AOPs also attacked these sites of CIP, and some similar products have been reported. Guo *et al.*<sup>13</sup> confirmed a series of products followed similar generation pathways like products A, D and E-1-1 during degradation of fluoroquinolone by UV/H<sub>2</sub>O<sub>2</sub>. In our previous study, UV/H<sub>2</sub>O<sub>2</sub> with multiple UV wavelengths was applied, and six similar products were determined.<sup>9</sup> In UV/TiO<sub>2</sub> systems, two mechanisms, including ·OH oxidation and direct degradation by the oxidative holes on TiO<sub>2</sub>, were proposed.<sup>40</sup> Following these two pathways, some products generated by addition reactions were also determined. However, these mechanisms were not true for other AOPs. Dodd *et al.*<sup>36</sup> found that ozone induced transformations on the quinolone backbone and piperazine ring of CIP.

After further VUV treatment, some other small molecular organics may be generated. Their absence in our data may be attributed to the detection limitation of LC-HRMS systems.

Table 2 CIP organic intermediates in VUV treatments

Name	Product A-1	Product A-2	Product B	Product C-1 <sup>a</sup>	Product C-2
Proposed structure					
Molecular formula	C <sub>17</sub> H <sub>19</sub> N <sub>3</sub> O <sub>4</sub> , 330.1448	C <sub>17</sub> H <sub>19</sub> N <sub>3</sub> O <sub>5</sub> , 346.1397	C <sub>16</sub> H <sub>18</sub> N <sub>3</sub> O <sub>2</sub> , 304.1456	C <sub>17</sub> H <sub>18</sub> N <sub>3</sub> O <sub>4</sub> , 348.1354	C <sub>17</sub> H <sub>18</sub> N <sub>3</sub> O <sub>5</sub> , 364.1303
and [M + H] <sup>+</sup> : m/z	2.568	2.980	1.912	2.914, 3.094	3.332
Retention time (min)					
Extracted ion spectrum					
Name	Product C-3	Product D	Product E-1-1 <sup>a</sup>	Product E-1-2 <sup>a</sup>	Product E-2-1 <sup>a</sup>
Proposed structure					
Molecular formula	C <sub>17</sub> H <sub>20</sub> N <sub>3</sub> O <sub>3</sub> , 366.438	C <sub>13</sub> H <sub>16</sub> N <sub>3</sub> O <sub>3</sub> , 306.1248	C <sub>17</sub> H <sub>16</sub> N <sub>3</sub> O <sub>4</sub> , 346.1198	C <sub>17</sub> H <sub>16</sub> N <sub>3</sub> O <sub>5</sub> , 362.1147	C <sub>17</sub> H <sub>18</sub> N <sub>3</sub> O <sub>4</sub> , 348.1354
and [M + H] <sup>+</sup> : m/z	2.905	2.905	2.981, 3.197	2.589, 3.339, 3.501, 4.075	2.914, 3.094
Retention time (min)					
Extracted ion spectrum					

Table 2 (continued)

Name	Product A-1	Product A-2	Product B	Product C-1 <sup>a</sup>	Product C-2
Name Proposed structure	Product E-2-2 <sup>a</sup> 	Product E-2-3 <sup>a</sup> 	Product E-2-4 		
Molecular formula	C <sub>17</sub> H <sub>16</sub> FN <sub>3</sub> O <sub>3</sub> , 330.1248	C <sub>17</sub> H <sub>16</sub> FN <sub>3</sub> O <sub>4</sub> , 346.1198	C <sub>17</sub> H <sub>18</sub> FN <sub>3</sub> O <sub>5</sub> , 364.1303		
and [M + H] <sup>+</sup> : m/z	2.571, 2.914, 3.066	2.981, 3.197	3.332		
Retention time (min)					
Extracted ion spectrum					

Experimental conditions: solution temperature  $25 \pm 2$  °C, pH 6.5–7.2, [CIP]<sub>0</sub> = 3.02 μM, 254 nm UV irradiation intensity = 2.0 mW cm<sup>-2</sup>, 185 nm VUV irradiation intensity = 0.12 mW cm<sup>-2</sup>. <sup>a</sup> Retention time indicates the appearance time of the highest peak in the extracted ion spectrum. Some extracted ion spectra included several peaks which suggested isomers with the same molecular formula.

However, concentrations of NO<sub>3</sub><sup>-</sup> and F<sup>-</sup> increased as the reaction proceeded (Fig. S3†), confirming the transformations of N and F in CIP. Generally, hydroxylation was the predominant reaction, and further additions, substitutions and cleavages resulted in gradual transformation of CIP.

### 3.4. Toxicology

Two parameters, ROS and apoptosis, were used to evaluate the variation of CIP toxicity during VUV treatment. ROS are natural chemical species with high reactivity, including superoxides, peroxides, hydroxyl radicals and singlet oxygen. ROS can result in significant damage of cell structures and reduction of biomolecule activities. The levels of ROS in the cells under exposure to degradation intermediates were higher than those in the cells exposed to CIP (Fig. 4a). The trend of the ROS level was consistent with the relative intensity variations of products A-1, B, C-1, D and E-2-1. These products all have hydroxyl addition or replacement, suggesting that the simple hydroxylation of CIP may increase its toxicity.

To reveal whether the increasing ROS caused cell lethality, cellular apoptosis was investigated. Apoptosis is a programmed process of cell death that is initiated by the sensation of cell stresses or signals from other cells. Based on the flow cytometer data, the cells were classified into live, early apoptosis, late apoptosis and dead cells. Apoptosis cannot stop after it begins, thus, the cells in the early and late stages of apoptosis will finally die. Their variation tendencies are presented in Fig. 4b. In the early stage (0–30 min of VUV treatment), a percentage of the live cells decreased while the apoptosis and dead cells increased. Of note, the highest percentage of apoptosis was observed at 30 min, which was consistent with the highest ROS. These results clarified that the increasing ROS directly induced cellular death. Most products, especially the simple hydroxylated products from CIP presented an increasing tendency during the early stage (0–60 min; Fig. 3). These apoptosis data confirmed that the toxicity of these incomplete degradation products in the early stage was higher than that of CIP. Furthermore, the intensities of these products decreased during 60–180 min, suggesting that they may be transformed into further products or small molecules. The percentage of live cells increased gradually during 30–180 min, thus, these further products may have lower toxicity. Although 180 min of VUV treatment did not completely mineralize and detoxify CIP, the downward percentage of apoptosis still indicated the decreasing toxicity of intermediates as the VUV treatment proceeded.

### 3.5. Influence factors

The reaction using 0.06 mW cm<sup>-2</sup> intensity was selected as the control group in the following influence factor experiments. Variation of pH values had a significant effect on VUV (Fig. 5a). Under different pH values (3.0–11.0), the *k*<sub>app</sub> varied from  $1.42 \times 10^{-3}$  s<sup>-1</sup> to  $4.91 \times 10^{-3}$  s<sup>-1</sup> and reached a

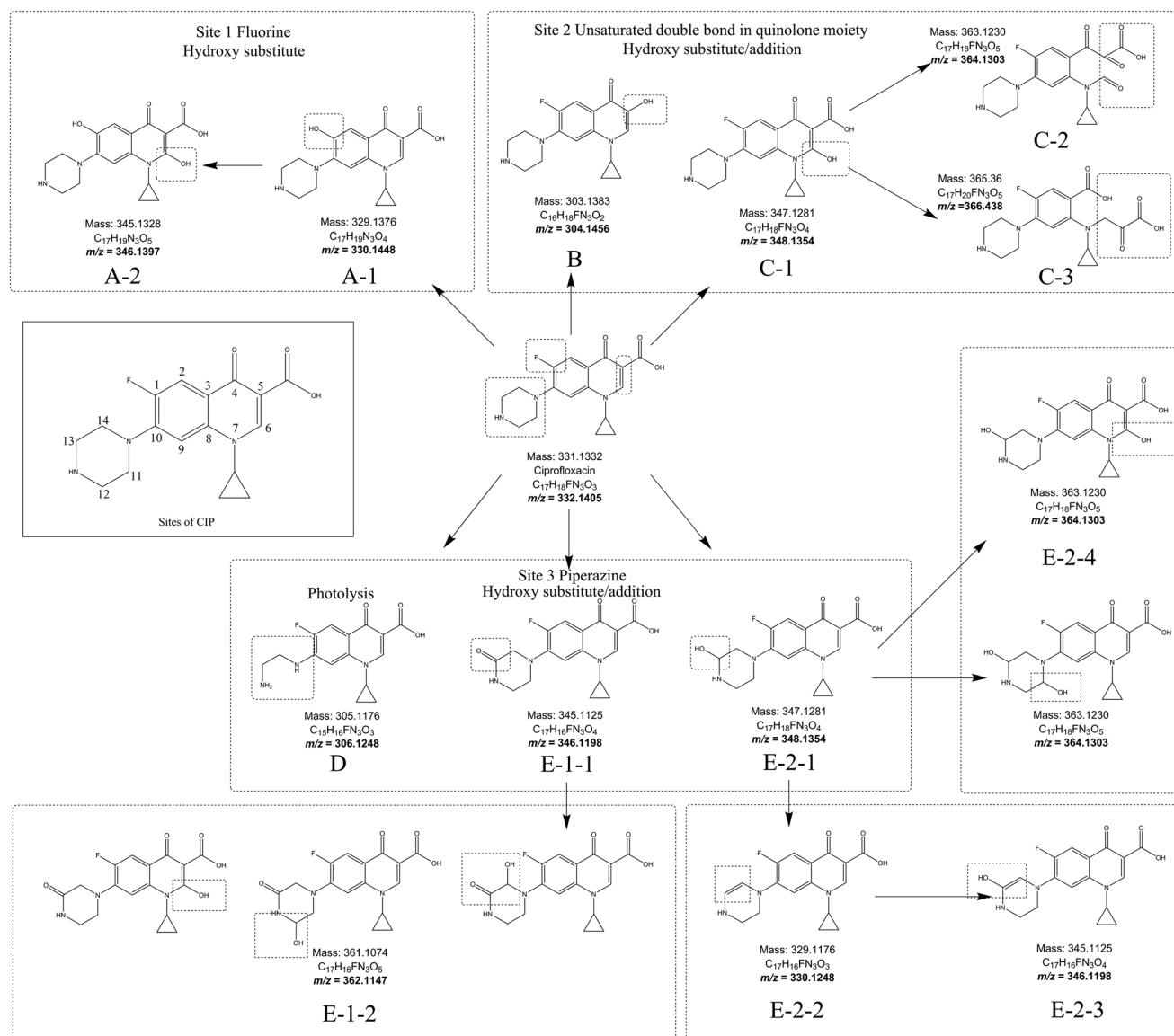
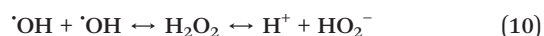


Fig. 2 Proposed generation pathways of the degradation products from CIP in the VUV system. Experimental conditions: solution temperature  $25 \pm 2$  °C, pH 6.5–7.2,  $[CIP]_0 = 3.02 \mu\text{M}$ , 254 nm UV irradiation intensity =  $2.0 \text{ mW cm}^{-2}$ , 185 nm VUV irradiation intensity =  $0.12 \text{ mW cm}^{-2}$ .

maximum at pH 7.0. It seems that the optimal reaction solution for CIP degradation in the VUV system was the neutral condition, which would be beneficial for actual water treatments. Generally, variation of pH affects the electronic charge values of some contaminants, especially quinolone.<sup>41</sup> CIP has zwitterionic functional groups, namely, a piperazine moiety with positive charge and a carboxyl group with negative charge. In the acid or alkaline solutions, CIP exists in its protonated or deprotonated form, and only at neutral pH can CIP reach the equipotential points.<sup>36</sup> Furthermore, neutral CIP was more susceptible to  $\cdot\text{OH}$ , resulting in higher oxidation reaction efficiencies. The  $pK_a$  of  $\text{H}_2\text{O}_2$  is close to 11,<sup>42</sup> thus, the formation of  $\text{HO}_2^-$  was promoted, reducing the steady-state concentration of  $\cdot\text{OH}$  (eqn (10)). Of note, the self-decomposition rate constants of  $\text{H}_2\text{O}_2$  were reported to be  $2.29 \times 10^{-2} \text{ min}^{-1}$  and  $7.40 \times 10^{-2} \text{ min}^{-1}$  at pH = 7.0

and 10.5, respectively (eqn (11)), suggesting that more  $\text{H}_2\text{O}_2$  decomposes into  $\text{H}_2\text{O}$  and  $\text{O}_2$  under alkaline conditions.<sup>43</sup> Furthermore,  $\text{OH}^-$  has a high  $\epsilon$  at 185 nm ( $3039 \pm 206 \text{ M}^{-1} \text{ cm}^{-1}$ ), impeding the VUV irradiation. Therefore, the degradation efficiency of CIP under alkaline conditions was inhibited severely.



To evaluate the effect of NOM, HA with a concentration of 2.5, 10, 25 and  $100 \text{ mg L}^{-1}$  was added, and increasing inhibition was observed (Fig. 5b). The  $k_{\text{app}}$  decreased from  $4.91 \times 10^{-3} \text{ s}^{-1}$  to  $1.39 \times 10^{-3} \text{ s}^{-1}$ . NOM can impede the propagation of UV and VUV photons and reduce the generation efficiency

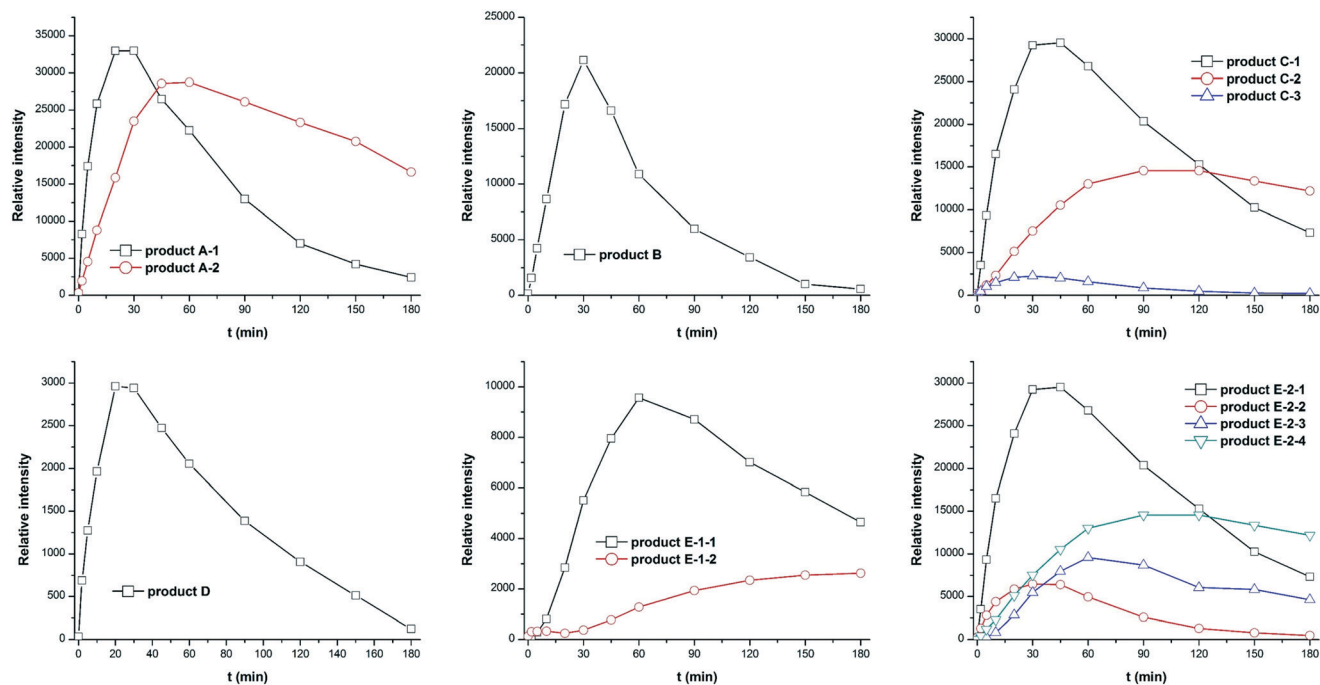


Fig. 3 Evolution curves of the degradation products. Experimental conditions: solution temperature  $25 \pm 2$  °C, pH 6.5–7.2,  $[CIP]_0 = 3.02 \mu\text{M}$ , 254 nm UV irradiation intensity =  $2.0 \text{ mW cm}^{-2}$ , 185 nm VUV irradiation intensity =  $0.12 \text{ mW cm}^{-2}$ .

of  $\cdot\text{OH}$ . Furthermore, HA can consume  $\cdot\text{OH}$ , which further reduces the degradation efficiency of CIP. Of note, the HA effect on the VUV system was slight with low concentration ( $<25 \text{ mg L}^{-1}$ ).

Anions are also important influence factors for the UV-based treatments, because they are potential inhibitors for VUV processes. The effects of  $\text{Cl}^-$ ,  $\text{NO}_3^-$ ,  $\text{HCO}_3^-$ ,  $\text{SO}_4^{2-}$  and  $\text{H}_2\text{PO}_4^-$  were tested.  $\text{Cl}^-$ ,  $\text{NO}_3^-$  and  $\text{HCO}_3^-$  had inhibition on

the CIP degradation (Fig. 5), as  $k_{\text{app}}$  decreased after adding these anions. Two mechanisms, including VUV screening ( $\epsilon$  at 185 nm, Table S2<sup>†</sup>) and  $\cdot\text{OH}$  scavenging ( $k_{\text{OH}}$ , Table S3<sup>†</sup>), may contribute to the inhibition synchronously. According to the Lambert–Beer law, the percentage of 185 nm photons absorbed by a particular constituent in the CIP solution with different kinds and concentrations of the anions was calculated using eqn (6). Both  $\text{NO}_3^-$  and  $\text{Cl}^-$  have a high  $\epsilon$  at 185

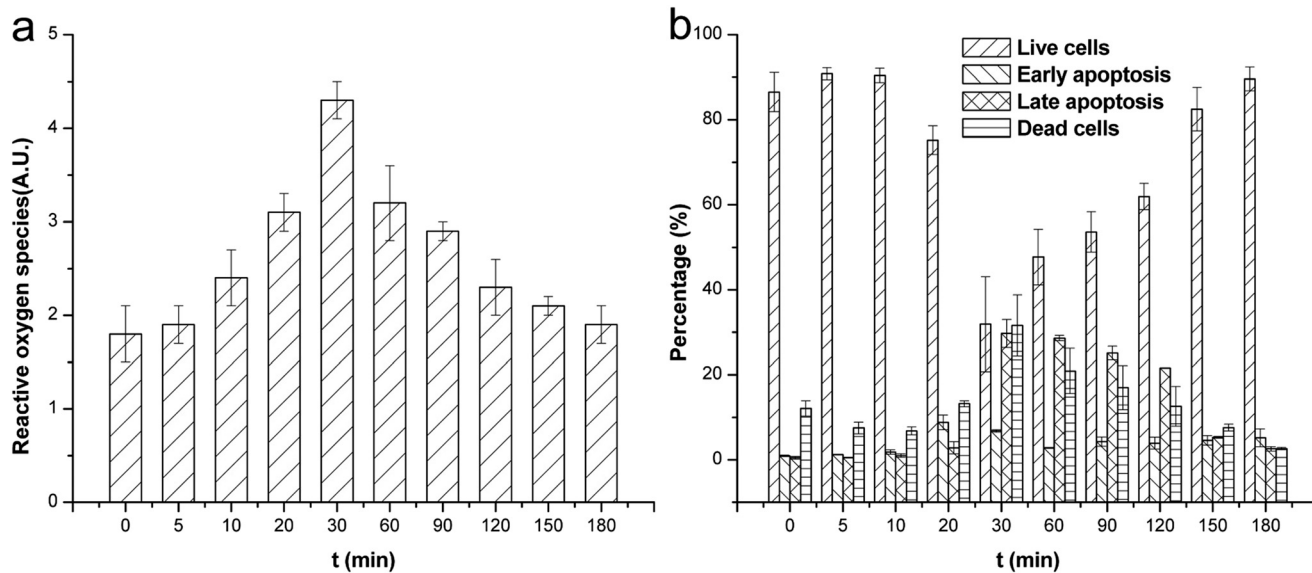
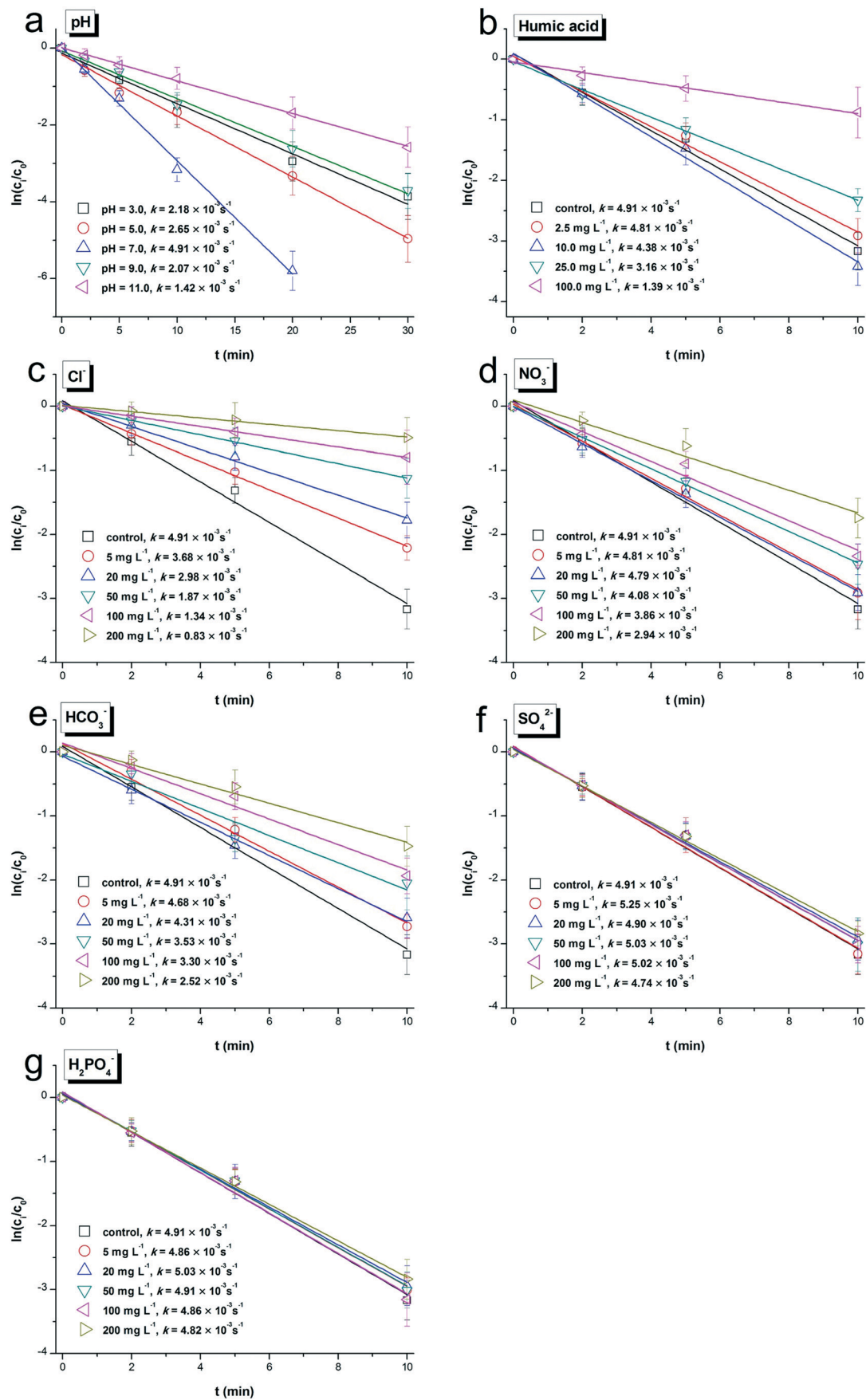


Fig. 4 Reactive oxygen species (a) and cellular apoptosis (b) in the cells exposed to the stresses from CIP and its intermediates. Experimental conditions: solution temperature  $25 \pm 2$  °C, pH 6.5–7.2,  $[CIP]_0 = 3.02 \mu\text{M}$ , 254 nm UV irradiation intensity =  $2.0 \text{ mW cm}^{-2}$ , 185 nm VUV irradiation intensity =  $0.12 \text{ mW cm}^{-2}$ . Experiment was carried out in triplicate and the error bars represent the standard error of the mean.



**Fig. 5** Degradation of CIP under different influence factors: (a) pH, (b) humic acid, (c) Cl<sup>-</sup>, (d) NO<sub>3</sub><sup>-</sup>, (e) HCO<sub>3</sub><sup>-</sup>, (f) SO<sub>4</sub><sup>2-</sup>, and (g) H<sub>2</sub>PO<sub>4</sub><sup>-</sup>. Experimental conditions: solution temperature 25 ± 2 °C, pH 6.5–7.2 (if not specified), [CIP]<sub>0</sub> = 3.02 μM, 254 nm UV irradiation intensity = 1.0 mW cm<sup>-2</sup>, 185 nm VUV irradiation intensity = 0.06 mW cm<sup>-2</sup>. All the experiments were carried out in triplicate with error bars representing the standard error of the mean.

nm, thus, these two anions absorbed most of the 185 nm irradiation (up to 85% at 200 mg L<sup>-1</sup>), resulting in inhibition of the photolysis of H<sub>2</sub>O and lower  $\cdot$ OH yield (Fig. 5c and d). NO<sub>3</sub><sup>-</sup> has a low reaction rate constant with  $\cdot$ OH ( $1 \times 10^5$  M<sup>-1</sup> s<sup>-1</sup> (ref. 44)), and its inhibition was weaker. For HCO<sub>3</sub><sup>-</sup>, a high  $k_{\text{OH}}$  at  $8.5 \times 10^8$  M<sup>-1</sup> s<sup>-1</sup> and a low  $\epsilon$  at  $464 \pm 64$  M<sup>-1</sup> cm<sup>-1</sup> at 185 nm contributed to its relative slight inhibition on VUV (Fig. 5e). In contrast, both SO<sub>4</sub><sup>2-</sup> and H<sub>2</sub>PO<sub>4</sub><sup>-</sup> had negligible effects (Fig. 5f and g). For example, H<sub>2</sub>PO<sub>4</sub><sup>-</sup> has a low  $\epsilon$  ( $344 \pm 38$  M<sup>-1</sup> cm<sup>-1</sup>) and a low reaction rate with  $\cdot$ OH ( $2.0 \times 10^4$  M<sup>-1</sup> s<sup>-1</sup>), resulting in its weak effect on CIP degradation under VUV irradiation. In general, investigating the effects of other constituents on the VUV system should take into account both VUV screening and  $\cdot$ OH scavenging capacities.

### 3.6. Cost evaluation

To evaluate the energy consumption of the VUV system, electrical energy per order (EE/O) analysis was applied. EE/O is defined as the electrical energy (kW h) required to degrade a contaminant by an order of magnitude in a 1 cm<sup>3</sup> matrix, and the relative result is presented in Table S4.† Detailed calculations can be found in our previous study.<sup>45</sup> The EE/O value was 0.006 kW h m<sup>-3</sup> per order in the VUV system under pH = 7.0 (control group). In the influence factor experiments, most EE/O values increased. Strong acidic (pH = 3.0) and strong alkaline (pH = 11.0) conditions increased the EE/O values to 0.014 and 0.021 kW h m<sup>-3</sup> per order, respectively. As the HA addition increased to 100 mg L<sup>-1</sup>, EE/O increased from 0.006 kW h m<sup>-3</sup> per order to 0.022 kW h m<sup>-3</sup> per order. The presence of anions also resulted in increasing EE/O. Of note, H<sub>2</sub>PO<sub>4</sub><sup>-</sup> and SO<sub>4</sub><sup>2-</sup> had slight effects on EE/O. These results suggested that the reaction conditions for CIP degradation by VUV should be maintained in neutral pH, and the presence of HA and some anions increased the energy cost.

## 4. Conclusion

Transformation mechanisms of CIP under VUV treatment involved 185 nm photolysis, 254 nm photolysis and  $\cdot$ OH oxidation, with a reaction rate constant  $k_{\text{OH-CIP}}$  at  $(8.6 \pm 0.8) \times 10^9$  M<sup>-1</sup> s<sup>-1</sup>. Five series of hydroxylated products were generated as the result of radical-based addition and substitution of CIP during the early stage of VUV treatment. Toxicity analysis revealed that these early stage products had higher toxicity than CIP or their further oxidized products. Variable pH values and natural organic matter/anions affected the degradation efficiency of CIP, while VUV screening and  $\cdot$ OH scavenging capacities were two key inhibition mechanisms. The VUV treatment using a low-pressure mercury VUV lamp induced radical-based oxidation of CIP, and it will be a promising treatment method for removing CIP from water.

## Conflicts of interest

There are no conflicts to declare.

## Acknowledgements

This project was supported by the National Natural Science Foundation of China (Grant No. 51778270) and the Fundamental Research Funds for the Central Universities (Grant No. 21617448 and 17817020).

## References

- 1 M. Seifrtova, L. Novakova, C. Lino, A. Pena and P. Solich, An overview of analytical methodologies for the determination of antibiotics in environmental waters, *Anal. Chim. Acta*, 2009, **649**, 158–179.
- 2 S. Zorita, L. Martensson and L. Mathiasson, Occurrence and removal of pharmaceuticals in a municipal sewage treatment system in the south of Sweden, *Sci. Total Environ.*, 2009, **407**, 2760–2770.
- 3 A. L. Batt, S. Kim and D. S. Aga, Comparison of the occurrence of antibiotics in four full-scale wastewater treatment plants with varying designs and operations, *Chemosphere*, 2007, **68**, 428–435.
- 4 E. M. Golet, I. Xifra, H. Siegrist, A. C. Alder and W. Giger, Environmental exposure assessment of fluoroquinolone antibacterial agents from sewage to soil, *Environ. Sci. Technol.*, 2003, **37**, 3243–3249.
- 5 I. Michael, L. Rizzo, C. S. McArdell, C. M. Manaia, C. Merlin, T. Schwartz, C. Dagot and D. Fatta-Kassinos, Urban wastewater treatment plants as hotspots for the release of antibiotics in the environment: A review, *Water Res.*, 2013, **47**, 957–995.
- 6 F. Adachi, A. Yamamoto, K. I. Takakura and R. Kawahara, Occurrence of fluoroquinolones and fluoroquinolone-resistance genes in the aquatic environment, *Sci. Total Environ.*, 2013, **444**, 508–514.
- 7 L. Aristilde, A. Melis and G. Sposito, Inhibition of photosynthesis by a fluoroquinolone antibiotic, *Environ. Sci. Technol.*, 2010, **44**, 1444–1450.
- 8 M. Li, D. B. Wei, H. M. Zhao and Y. G. Du, Genotoxicity of quinolones: Substituents contribution and transformation products QSAR evaluation Using 2D and 3D models, *Chemosphere*, 2014, **95**, 220–226.
- 9 H. S. Ou, J. S. Ye, S. Ma, C. H. Wei, N. Y. Gao and J. Z. He, Degradation of ciprofloxacin by UV and UV/H<sub>2</sub>O<sub>2</sub> via multiple-wavelength ultraviolet light-emitting diodes: Effectiveness, intermediates and antibacterial activity, *Chem. Eng. J.*, 2016, **289**, 391–401.
- 10 V. J. Pereira, K. G. Linden and H. S. Weinberg, Evaluation of UV irradiation for photolytic and oxidative degradation of pharmaceutical compounds in water, *Water Res.*, 2007, **41**, 4413–4423.
- 11 I. Siminiceanu and M. M. Bobu, A comparative kinetic study of the ciprofloxacin degradation in water by several advanced oxidation processes, *Rev. Chim.*, 2006, **57**, 1205–1209.
- 12 O. S. Keen and K. G. Linden, Degradation of antibiotic activity during UV/H<sub>2</sub>O<sub>2</sub> advanced oxidation and photolysis

- in wastewater effluent, *Environ. Sci. Technol.*, 2013, **47**, 13020–13030.
- 13 H. G. Guo, N. Y. Gao, W. H. Chu, L. Li, Y. J. Zhang, J. S. Gu and Y. L. Gu, Photochemical degradation of ciprofloxacin in UV and UV/H<sub>2</sub>O<sub>2</sub> process: kinetics, parameters, and products, *Environ. Sci. Pollut. Res.*, 2013, **20**, 3202–3213.
  - 14 C. C. Lin and M. S. Wu, Degradation of ciprofloxacin by UV/S<sub>2</sub>O<sub>8</sub><sup>2-</sup> process in a large photoreactor, *J. Photochem. Photobiol., A*, 2014, **285**, 1–6.
  - 15 E. A. Serna-Galvis, F. Ferraro, J. Silva-Agrede and R. A. Torres-Palma, Degradation of highly consumed fluoroquinolones, penicillins and cephalosporins in distilled water and simulated hospital wastewater by UV<sub>254</sub> and UV<sub>254</sub>/persulfate processes, *Water Res.*, 2017, **122**, 128–138.
  - 16 J. S. Ye, J. Liu, H. S. Ou and L. L. Wang, Degradation of ciprofloxacin by 280 nm ultraviolet-activated persulfate: Degradation pathway and intermediate impact on proteome of *Escherichia coli*, *Chemosphere*, 2016, **165**, 311–319.
  - 17 W. H. Li, C. S. Guo, S. Su and J. Xu, Photodegradation of four fluoroquinolone compounds by titanium dioxide under simulated solar light irradiation, *J. Chem. Technol. Biotechnol.*, 2012, **87**, 643–650.
  - 18 M. S. Peres, M. G. Maniero and J. R. Guimaraes, Photocatalytic degradation of ofloxacin and evaluation of the residual antimicrobial activity, *Photochem. Photobiol. Sci.*, 2015, **14**, 556–562.
  - 19 P. Verma and S. K. Samanta, Degradation kinetics of pollutants present in a simulated wastewater matrix using UV/TiO<sub>2</sub> photocatalysis and its microbiological toxicity assessment, *Res. Chem. Intermed.*, 2017, **43**, 6317–6341.
  - 20 G. E. Imoberdorf and M. Mohseni, Experimental study of the degradation of 2,4-D induced by vacuum-UV radiation, *Water Sci. Technol.*, 2011, **63**, 1427–1433.
  - 21 T. Oppenlander and S. Gliese, Mineralization of organic micropollutants (homologous alcohols and phenols) in water by vacuum-UV-oxidation (H<sub>2</sub>O-VUV) with an incoherent xenon-excimer lamp at 172 nm, *Chemosphere*, 2000, **40**, 15–21.
  - 22 H. Shirayama, Y. Tohezo and S. Taguchi, Photodegradation of chlorinated hydrocarbons in the presence and absence of dissolved oxygen in water, *Water Res.*, 2001, **35**, 1941–1950.
  - 23 Y. R. Gu, T. Z. Liu, H. J. Wang, H. L. Han and W. Y. Dong, Hydrated electron based decomposition of perfluorooctane sulfonate (PFOS) in the VUV/sulfite system, *Sci. Total Environ.*, 2017, **607**, 541–548.
  - 24 C. Duca, G. Imoberdorf and M. Mohseni, Effects of inorganics on the degradation of micropollutants with vacuum UV (VUV) advanced oxidation, *J. Environ. Sci. Health, Part A: Toxic/Hazard. Subst. Environ. Eng.*, 2017, **52**, 524–532.
  - 25 G. Imoberdorf and M. Mohseni, Kinetic study and modeling of the vacuum-UV photoinduced degradation of 2,4-D, *Chem. Eng. J.*, 2012, **187**, 114–122.
  - 26 M. K. Li, Z. M. Qiang, P. Hou, J. R. Bolton, J. H. Qu, P. Li and C. Wang, VUV/UV/Chlorine as an Enhanced Advanced Oxidation Process for Organic Pollutant Removal from Water: Assessment with a Novel Mini-Fluidic VUV/UV Photo-reaction System (MVPS), *Environ. Sci. Technol.*, 2016, **50**, 5849–5856.
  - 27 M. K. Li, Z. M. Qiang, C. Pulgarin and J. Kiwi, Accelerated methylene blue (MB) degradation by Fenton reagent exposed to UV or VUV/UV light in an innovative micro photo-reactor, *Appl. Catal., B*, 2016, **187**, 83–89.
  - 28 M. K. Li, C. Wang, M. L. Yau, J. R. Bolton and Z. M. Qiang, Sulfamethazine degradation in water by the VUV/UV process: Kinetics, mechanism and antibacterial activity determination based on a mini-fluidic VUV/UV photoreaction system, *Water Res.*, 2017, **108**, 348–355.
  - 29 K. Zoschke, H. Bornick and E. Worch, Vacuum-UV radiation at 185 nm in water treatment - A review, *Water Res.*, 2014, **52**, 131–145.
  - 30 M. M. Huber, S. Canonica, G. Y. Park and U. Von Gunten, Oxidation of pharmaceuticals during ozonation and advanced oxidation processes, *Environ. Sci. Technol.*, 2003, **37**, 1016–1024.
  - 31 Y. Li, C. S. Li, H. M. Qin, M. Yang, J. S. Ye, Y. Long and H. S. Ou, Proteome and phospholipid alteration reveal metabolic network of *Bacillus thuringiensis* under triclosan stress, *Sci. Total Environ.*, 2018, **615**, 508–516.
  - 32 W. Y. Han, P. Y. Zhang, W. P. Zhu, J. J. Yin and L. S. Li, Photocatalysis of p-chlorobenzoic acid in aqueous solution under irradiation of 254 nm and 185 nm UV light, *Water Res.*, 2004, **38**, 4197–4203.
  - 33 V. J. Pereira, H. S. Weinberg, K. G. Linden and P. C. Singer, UV degradation kinetics and modeling of pharmaceutical compounds in laboratory grade and surface water via direct and indirect photolysis at 254 nm, *Environ. Sci. Technol.*, 2007, **41**, 1682–1688.
  - 34 F. Yuan, C. Hu, X. X. Hu, D. B. Wei, Y. Chen and J. H. Qu, Photodegradation and toxicity changes of antibiotics in UV and UV/H<sub>2</sub>O<sub>2</sub> process, *J. Hazard. Mater.*, 2011, **185**, 1256–1263.
  - 35 T. C. An, H. Yang, G. Y. Li, W. H. Song, W. J. Cooper and X. P. Nie, Kinetics and mechanism of advanced oxidation processes (AOPs) in degradation of ciprofloxacin in water, *Appl. Catal., B*, 2010, **94**, 288–294.
  - 36 M. C. Dodd, M. O. Buffle and U. Von Gunten, Oxidation of antibacterial molecules by aqueous ozone: Moiety-specific reaction kinetics and application to ozone-based wastewater treatment, *Environ. Sci. Technol.*, 2006, **40**, 1969–1977.
  - 37 W. H. M. Abdelraheem, X. He, X. Duan and D. D. Dionysiou, Degradation and mineralization of organic UV absorber compound 2-phenylbenzimidazole-5-sulfonic acid (PBSA) using UV-254nm/H<sub>2</sub>O<sub>2</sub>, *J. Hazard. Mater.*, 2015, **282**, 233–240.
  - 38 W. H. M. Abdelraheem, M. K. Patil, M. N. Nadagouda and D. D. Dionysiou, Hydrothermal synthesis of photoactive nitrogen- and boron- codoped TiO<sub>2</sub> nanoparticles for the treatment of bisphenol A in wastewater: Synthesis, photocatalytic activity, degradation byproducts and reaction pathways, *Appl. Catal., B*, 2019, **241**, 598–611.
  - 39 M. Y. Kilic, W. H. Abdelraheem, X. He, K. Kestioglu and D. D. Dionysiou, Photochemical treatment of tyrosol, a model phenolic compound present in olive mill wastewater,

- by hydroxyl and sulfate radical-based advanced oxidation processes (AOPs), *J. Hazard. Mater.*, 2018, in press.
- 40 P. Villegas-Guzman, S. Oppenheimer-Barrot, J. Silva-Agredo and R. A. Torres-Palma, Comparative evaluation of photochemical AOPs for ciprofloxacin degradation: elimination in natural waters and analysis of pH effect, primary degradation by-products, and the relationship with the antibiotic activity, *Water, Air, Soil Pollut.*, 2017, **228**, 209–223.
- 41 W. B. Yang, Y. P. Lu, F. F. Zheng, X. X. Xue, N. Li and D. M. Liu, Adsorption behavior and mechanisms of norfloxacin onto porous resins and carbon nanotube, *Chem. Eng. J.*, 2012, **179**, 112–118.
- 42 J. C. Crittenden, S. Hu, D. W. Hand and S. A. Green, A kinetic model for H<sub>2</sub>O<sub>2</sub>/UV process in a completely mixed batch reactor, *Water Res.*, 1999, **33**, 2315–2328.
- 43 W. Chu, Modeling the quantum yields of herbicide 2,4-D decay in UV/H<sub>2</sub>O<sub>2</sub> process, *Chemosphere*, 2001, **44**, 935–941.
- 44 M. C. Gonzalez and A. M. Braun, VUV photolysis of aqueous solutions of nitrate and nitrite, *Res. Chem. Intermed.*, 1995, **21**, 837–859.
- 45 J. S. Ye, J. Liu, C. S. Li, P. L. Zhou, S. Wu and H. S. Ou, Heterogeneous photocatalysis of tris(2-chloroethyl) phosphate by UV/TiO<sub>2</sub>: Degradation products and impacts on bacterial proteome, *Water Res.*, 2017, **124**, 29–38.